J Neurophysiol 99: 2602–2616, 2008.
First published March 12, 2008; doi:10.1152/jn.01379.2007.

The Brain Stem Saccadic Burst Generator Encodes Gaze in Three-Dimensional Space

Marion R. Van Horn, Pierre A. Sylvestre, and Kathleen E. Cullen
Aerospace Medical Research Unit, Department of Physiology, McGill University, Montreal, Province of Quebec, Canada

Submitted 20 December 2007; accepted in final form 11 March 2008

Van Horn MR, Sylvestre PA, Cullen, KE. The brain stem saccadic burst generator encodes gaze in three-dimensional space. *J Neurophysiol* 99: 2602–2616, 2008. First published March 12, 2008; doi:10.1152/jn.01379.2007. When we look between objects located at different depths the horizontal movement of each eye is different from that of the other, yet temporally synchronized. Traditionally, a vergence-specific neuronal subsystem, independent from other oculomotor subsystems, has been thought to generate all eye movements in depth. However, recent studies have challenged this view by unmasking interactions between vergence and saccadic eye movements during disconjugate saccades. Here, we combined experimental and modeling approaches to address whether the premotor command to generate disconjugate saccades originates exclusively in "vergence centers." We found that the brain stem burst generator, which is commonly assumed to drive only the conjugate component of eye movements, carries substantial vergence-related information during disconjugate saccades. Notably, facilitated vergence velocities during disconjugate saccades were synchronized with the burst onset of excitatory and inhibitory brain stem saccadic burst neurons (SBNs). Furthermore, the time-varying discharge properties of the majority of SBNs (>70%) preferentially encoded the dynamics of an individual eye during disconjugate saccades. When these experimental results were implemented into a computer-based simulation, to further evaluate the contribution of the saccadic burst generator in generating disconjugate saccades, we found that it carries all the vergence drive that is necessary to shape the activity of the abducens motoneurons to which it projects. Taken together, our results provide evidence that the premotor commands from the brain stem saccadic circuitry, to the target motoneurons, are sufficient to ensure the accurate control shifts of gaze in three dimensions.

INTRODUCTION

Precisely coordinating the movements of our eyes is critical for achieving an accurate visual perception in a three-dimensional world. In particular, unequal yet tightly controlled rotations of the eyes must be programmed whenever the point of fixation is shifted between objects located at different depths. The difference between the rotations of the eyes is referred to as a vergence eye movement. Traditionally saccadic and vergence eye movements are considered as two distinct subclasses of eye movements generated by largely distinct neuronal circuitries. However, numerous studies have provided results that argue against this view. Vergence velocities are greater than what would be predicted by a linear summation of a conjugate saccade with a saccade-free vergence movement, while conjugate velocities are decreased (Busettini and Mays 2003, 2005a; Collewijn et al. 1995, 1997; Enright 1984, 1992; Erkelens et al. 1989; Kenyon et al. 1980; Kumar et al. 2005; Maxwell and King 1992; Ono et al. 1978; Oohira 1993; Zee et al. 1992). Moreover, the amount of vergence facilitation is dependent on peak saccadic velocity (Busettini and Mays 2005a).

How the brain facilitates vergence eye movements during disconjugate saccades remains a topic of debate. On the one hand, it had been proposed that vergence facilitation occurs because inhibitory omnipause neurons in the dorsal raphe nucleus simultaneously gate activity of distinct saccadic and vergence pathways (Mays and Gamlin 1995; Zee et al. 1992). On the other hand, a series of studies have provided evidence that the saccadic premotor pathway plays a role in facilitating vergence shifts by encoding integrated conjugate and vergence premotor commands. For example, although stimulation of the superior colliculus generally elicits conjugate saccades (Schiller and Stryker 1972), it can disrupt vergence movements when applied midflight during a disconjugate saccade (Chaturvedi and Van Gisbergen 1999, 2000). In addition, premotor saccadic burst neurons (SBNs) show monocular tuning (i.e., a combination of conjugate and vergence signals) during disconjugate saccades (Zhou and King 1998). Although these findings are consistent with the hypothesis that the saccadic circuitry plays a role in facilitating vergence shifts, they cannot rule out the alternative possibility that the overall contribution of the saccadic circuitry is relatively unimportant compared with that of the vergence subsystem. Notably, the most recent proposal is that SBNs exclusively encode conjugate saccadic dynamics that interact with the vergence subsystem (Busettini and Mays 2005b).

Here we investigated whether the saccadic burst generator is strictly a "conjugate" premotor control pathway to resolve whether the saccadic pathway encodes sufficient vergence-related information to drive disconjugate saccades. We recorded from single neurons in the brain stem saccadic burst generator during disconjugate saccades and found that they dynamically encode vergence-related information. Using simulation, we further show that this command signal from the premotor saccadic circuitry is in fact sufficient to drive the target extraocular motoneurons during disconjugate saccades. Accordingly, a separate vergence subsystem is not required to control the abducens nucleus (ABN) during disconjugate saccades. Overall, our results strongly suggest that the drive from the saccadic burst generator is essential for the control of gaze in three dimensions.

Address for reprint requests and other correspondence: K. E. Cullen, McIntyre Medical Research Building, Room 1220, 3655 Prom. Sir William Osler, Montreal, PQ, Canada H3G 1Y6 (E-mail: kathleen.cullen@mcgill.ca).

The costs of publication of this article were defrayed in part by the payment of page charges. The article must therefore be hereby marked "*advertisement*" in accordance with 18 U.S.C. Section 1734 solely to indicate this fact.

METHODS

Animals and surgical procedures

Two rhesus monkeys (*Macaca mulatta*) were prepared for chronic extracellular recording under aseptic conditions. All procedures were approved by the McGill University Animal Care Committee and were in compliance with the guidelines of the Canadian Council on Animal Care. The surgical preparation has been described previously (Sylvestre and Cullen 1999). Briefly, using aseptic techniques and isoflurane anesthesia (2–3%, to effect), we implanted several stainless steel screws into the skull and attached a stainless steel recording chamber and a post for head restraint to these screws with dental cement. In the same procedure, a 17- to 18-mm-diameter eye coil, consisting of three loops of Teflon-coated stainless steel wire, was implanted in each eye beneath the conjunctiva (Judge et al. 1980). Following the surgery, the animals were administered buprenorphine [0.01 mg/kg, administered intramuscularly (im)] for postoperative analgesia and the antibiotic cephazolin (Ancef; 25 mg/kg im, for 5 days). Animals were given ≥2 wk to recover from the surgery before experiments began.

Behavioral paradigms

Head-restrained monkeys were seated in a primate chair that rested on a vestibular turntable and were trained to fixate targets in a dimly lit room for a juice reward. Monkeys were required to fixate light targets for 1–3 s to receive a reward. The timing and location of target illumination, data acquisition, and on-line data displays were controlled using REX (Real-time Experimentation System), a UNIX-based real-time acquisition system (Hayes et al. 1982). Neuronal responses were recorded during three types of eye movements: *1*) conjugate saccades; *2*) disconjugate saccades; and *3*) smooth, saccade-free vergence. Figure 1 illustrates an example of each of these three types of eye movements where the right eye moved approximately the same amount, in the same direction.

First, to elicit conjugate eye movements (i.e., ΔVergence <2°; Fig. 1*A*), a red HeNe laser was projected via a system of two galvanometer-controlled mirrors onto a cylindrical screen (approximately isovergent) located 55 cm away from the monkey's head (<4° convergence). Ipsilaterally and contralaterally directed conjugate saccades were elicited by stepping the target between horizontal positions (±5–30°), in 5° increments, in predictable and unpredictable sequences. In addition, conjugate smooth pursuit eye movements were obtained using a sinusoidally moving laser target (40°/s peak velocity, 0.5 Hz).

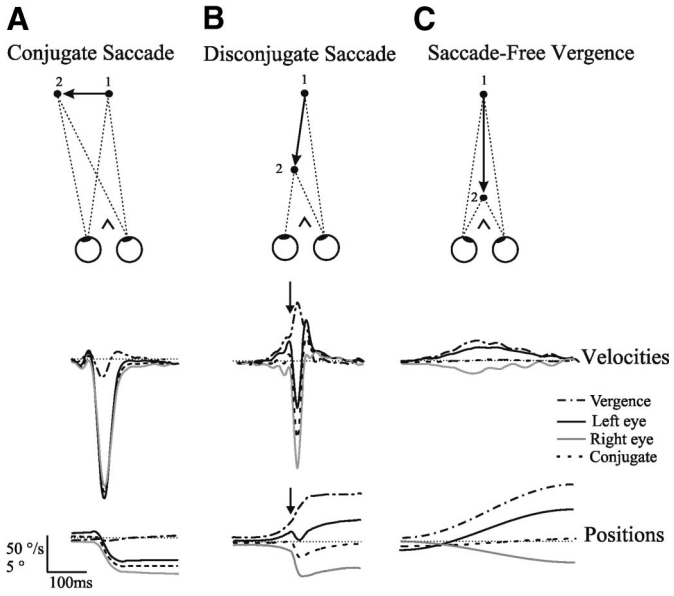

FIG. 1. Example of a conjugate saccade (*A*), a disconjugate saccade (*B*), and smooth saccade-free vergence (*C*). Arrows in *B* denote when the onset of the saccade and the onset of vergence facilitation. Note that in each case the right eye is moving approximately the same amplitude (5° to the left) and that the final vergence amplitude in *B* and *C* is the same. The final vergence amplitude is reached much faster when a disconjugate saccade is made.

Second, a horizontal array of 16 computer-controlled red light-emitting diodes (LEDs) with intensities comparable to that of the laser target (see Sylvestre and Cullen 1999) was used in combination with the laser target to elicit disconjugate saccades (Fig. 1*B*). Disconjugate saccades were generated when the illuminated target changed from one of the close midsagittal LEDs to an eccentric (i.e., right or left of the midsagittal plane) laser target. During this paradigm, monkeys made disconjugate saccades with conjugate components 5–30° in amplitude in both directions and vergence components with amplitudes 4–13°. In addition, some LEDs were positioned in a configuration similar to the Müller paradigm to generate "monocular" saccades in which the movement of one eye is largely reduced (for comparable examples see Ramat et al. 1999). Finally, saccade-free vergence eye movements were also evoked by having monkeys look between four LEDs (convergence angles: 17, 12, 8, and 6°) and a laser target, aligned with the monkey's midsagittal plane (Fig. 1*C*). Neurons that burst during conjugate saccades, but also responded to conjugate sinusoidal smooth pursuit (40°/s peak velocity, 0.5 Hz) or cancellation of the vestibuloocular reflex (VORc; 40°/s peak velocity, 0.5 Hz), were not included in our sample.

Data acquisition procedures

Extracellular single-unit activity was recorded using high-impedance enamel-insulated tungsten microelectrodes (2- to 10-MΩ impedance; FHC, Bowdoinham, ME). Saccadic burst neurons ($n = 74$) were identified on-line based on their stereotypical discharge properties during eye movements (Cullen and Guitton 1997). Excitatory and inhibitory burst neurons (EBNs and IBNs, respectively) were distinguished based on their recording location relative to the ABN. EBNs were recorded in a small region extending 1–2 mm rostral to the ABN and 0.5–1.5 mm from the midline. IBNs were recorded in a region extending 0–2 mm caudal to the ABN and 0.5–1.5 mm from the midline. Both areas correspond to previous anatomical characterizations (Strassman et al. 1986a,b). A small sample of omnipause neurons (OPNs, $n = 10$) was also recorded. A neuron was considered to be sufficiently isolated only when individual action potential waveforms could be discriminated during saccades using a windowing circuit (Bak Electronics, Mount Airy, MD; see Fig. 1 in Sylvestre and Cullen 1999).

The magnetic search coil technique was used to record the horizontal and vertical positions of both eyes (Fuchs and Robinson 1966; Judge et al. 1980). Each eye coil signal was calibrated independently by having the monkey fixate, with one eye masked, a variety of targets at different horizontal eccentricities and depths. Position signals were low-pass filtered at 250 Hz (analog eight-pole Bessel filter) and sampled at 1 kHz. Because ocular saccades include very little power at >50 Hz (e.g., Cullen et al. 1996; Van Opstal et al. 1985; Zuber et al. 1968) eye position signals were further digitally filtered (with a 51st-order finite-impulse-response filter with a Hamming window and a cutoff at 125 Hz), before being differentiated to obtain eye velocity signals (using zero-phase forward and reverse digital filtering to prevent phase distortion). Targets, rewards, on-line data displays, and data acquisition were controlled using custom-designed algorithms developed in the REX environment (Hayes et al. 1982). Off-line analysis was performed in the Matlab programming environment (The MathWorks, Natick, MA).

Data analysis

In this report, the eyes are referred to as ipsilateral or contralateral based on their location relative to the recording site. Positive and

negative values correspond to positions right and left of the sagittal plane, respectively. We also describe eye movements in terms of conjugate [conjugate = (left eye + right eye)/2] and vergence (vergence = left eye − right eye) coordinates. Note that vergence positions are always positive, but vergence velocities can be either positive (convergence) or negative (divergence). For all saccades, the onset and offset were determined using a 20°/s conjugate velocity criterion. Analysis was limited to horizontal saccades, which were defined as movements having changes in vertical eye position <10% of the change in horizontal position. Conjugate saccades were defined as having changes in vergence angles <2°. Disconjugate saccades were selected for which one eye moved more than the other, generating vergence velocities >100°/s and mean intrasaccadic vergence shifts of 6.5 ± 1.1°. Moreover, only saccades for which both eyes moved in the same direction were used to limit the analysis to ON-direction responses. Conjugate and disconjugate data sets contained >40 saccades (average $N_{conj} = 45.8 \pm 6.9$; average $N_{disconj} = 44.1 \pm 5.9$ saccades). An equal number of converging and diverging saccades were included in the disconjugate data set to prevent biasing the parameter estimates. Many disconjugate saccades were accompanied by periods of slow vergence preceding or following the onset of the saccade. The onset and offset of these slower movements were determined using a 10°/s vergence velocity criterion. For our data set of pure vergence movements, analysis was restricted to periods of saccade-free vergence movements and smooth vergence responses for which changes in conjugate horizontal or vertical component were <10% of the change in vergence.

Dynamic analysis of BN firing rate

The linear optimization techniques used to quantify the dynamic sensitivity of a neuron to eye movements during conjugate saccades (Cullen and Guitton 1996, 1997; Sylvestre and Cullen 1999) and disconjugate saccades (Sylvestre et al. 2002, 2003) have been extensively described. Neuronal discharges were represented as a spike density function in which a Gaussian function (SD of 5 ms) was convolved with the spike train (Cullen and Guitton 1996, 1997; Sylvestre and Cullen 1999; Sylvestre et al. 2002). This Gaussian width effectively low-pass filtered burst neuron discharges so that the frequency content is comparable to the associated saccadic movement (Cullen et al. 1996). A neuron's saccadic lead time was determined using both a first-spike and a dynamic lead time (t_d) approach (Cullen and Guitton 1996).

The specific model structures used are reported in RESULTS. The goodness-of-fit of the data to each model was quantified using the variance-accounted-for (VAF = 1 − [var (mod − fr)/var (fr)], where mod represents the modeled firing rate and fr represents the actual firing rate). The VAF in linear models is equivalent to the square of the correlation coefficient (R^2) such that a model with a VAF of 0.64 provides as good a fit to the data as a linear regression analysis that yields a correlation coefficient of 0.80 (Cullen et al. 1996).

For each model parameter in the analysis of disconjugate saccades, we computed 95% confidence intervals using a nonparametric bootstrap approach (Carpenter and Bithell 2000; Crawford et al. 1998; Press 1997; Sokal et al. 1995) and used these confidence intervals to identify nonsignificant or identical model parameters (Sylvestre et al. 2002, 2003). If a confidence interval overlapped with zero the model was rerun with the nonsignificant term removed. The Bayesian information criterion (BIC; Schwarz 1978), which served as a "cost index," was calculated for each model estimation to quantitatively determine whether removing the term was justified. If the BIC did not change this indicated that a new model described the data as well as the more complex model, thereby justifying removal of the term.

Metric analysis of BN discharges

To compare our sample of EBNs and IBNs with those previously described in the literature, saccade-related burst activity was also characterized using classical metric-based analyses. The number of spikes (NOS) was defined as the total number of action potentials that a neuron produced during an associated saccade and burst duration was defined as the time between the onset and offset of the burst. For each neuron, standard linear regression techniques were used to describe the relationships between *1*) saccade duration and burst duration, *2*) total vergence duration and burst duration, *3*) saccade amplitude and NOS, and *4*) peak saccade velocity and firing rate.

During disconjugate saccades, the classic metric approaches were adapted to account for the movements of both eyes

$$NOS = b + z_i \Delta IE + z_c \Delta CE \quad (1)$$

$$FR_{max} = b + p_i \dot{IE}_{max} + p_c \dot{CE}_{max} \quad (2)$$

where b is the bias; z_i and z_c are the regression coefficients relating the number of spikes to ipsilateral (ΔIE) or contralateral saccade amplitude (ΔCE), respectively; p_i and p_c are the regression coefficients relating the peak firing rate to the peak velocity of the ipsilateral ($\dot{IE}$) and contralateral eye ($\dot{CE}$), respectively.

Quantification of ocular preference

First, to quantify the ocular preference (see Table 1), *Ratio* indices were defined as follows

$$Ratio = \frac{Smaller\ estimated\ parameter\ value}{Larger\ estimated\ parameter\ value}$$

For each neuron three ratio indices were calculated. The ratio of a given neuron's sensitivity to the velocity of each eye (estimated using the dynamic analysis) was used to compute $Ratio_{dyn}$. Ratios of the regression coefficients estimated using the metric-based relationships between NOS and movement amplitude (*Eq. 1*), and peak firing rate

TABLE 1. *Categories of ocular preferences*

Category	Criteria	Ratio Value	Subscript
Mono. ipsi.	Contra. eye par. = 0 Ipsi. eye par. ≠ 0	0	i
Mono. contra.	Ipsi. eye par. = 0 Contra. eye par. ≠ 0	0	c
Bino. ipsi.	Ipsi. eye par. > Contra. eye par. Ipsi. eye par. ≠ Contra. eye par. ≠ 0	−1 ≤ Ratio < 1, Ratio ≠ 0	i
Bino. contra.	Ipsi. eye par. < Contra. eye par. Ipsi. eye par. ≠ Contra. eye par. ≠ 0	−1 ≤ Ratio < 1, Ratio ≠ 0	c
Conj.	Ipsi. eye par. = Contra. eye par. Ipsi. eye par. ≠ Contra. eye par. ≠ 0	1	

Mono, monocular; Bino, binocular; Conj, conjugate; Ipsi, ipsilateral eye preference; Contra, contralateral eye preference; Par, parameter value. This table was reproduced from Sylvestre et al. (2003).

and velocity (*Eq. 2*) were used to compute $Ratio_{NOS}$ and $Ratio_{FRmax}$, respectively.

Second, to facilitate comparison between our sample of neurons to those of Zhou and King (1998), who used a NOS-based approach identical to that shown in *Eq. 1*, we computed an ocular index (OI) that was converted to a $Ratio_{NOS}$ index

$$OI = \frac{z_i - z_c}{z_i + z_c}$$

that we reorganized to

$$\frac{OI + 1}{1 - OI} = \frac{z_i}{z_c} = Ratio_{NOS}$$

where z_i and z_c are the regression coefficients relating the number of spikes to ipsilateral or contralateral saccade amplitude, respectively.

Parameter values were compared across neuron types (short- and long-lead EBNs and IBNs; see RESULTS), using a one-way ANOVA followed by a standard post hoc multiple comparison test. Briefly, this latter test computes a Student's *t*-test for all *k* permutations among the groups included in the ANOVA and uses the Dunn–Šidák method [where the significance level (α') of each *k t*-test is defined as $\alpha' = 1 - (1 - \alpha)^{1/k}$; $\alpha = 0.05$] to correct for the effect of multiple comparisons (Sokal and Rohlf 1995). To compare the frequency of distribution of different neuron types across categories of ocular preferences, we performed a χ^2 test on a contingency table (Wackerly et al. 1996). Note that the unequal binocular neurons were pooled in two categories for this analysis: unequal binocular with a preference for the ipsilateral eye or unequal binocular with a preference for the contralateral eye.

Simulation design

A computer-based simulation was implemented in which the discharges of saccadic burst neurons (present study) were combined with those of other saccade-related premotor neurons with known projections to the ABN (McConville et al. 1994; Roy and Cullen 2002, 2003; Scudder and Fuchs 1992; Sylvestre and Cullen 1999; Sylvestre et al. 2003). The discharge dynamics of abducens motoneurons were predicted based on the weighted sum of inputs from different premotor neuron types ($n = 8$). The following criteria were used in the simulation's design. First, all premotor neurons included were shown experimentally to project to the ABN (Langer et al. 1986; McFarland and Fuchs 1992; Scudder and Fuchs 1992; Strassman et al. 1986a,b). Second, the nature of each connection (i.e., excitatory or inhibitory) was determined experimentally (Scudder and Fuchs 1992; Scudder et al. 2002). Third, for each neuron type (including ABN neurons), mathematical descriptions obtained experimentally from populations of neurons were available to reconstruct average population discharges during different oculomotor behaviors (see Supplemental Table S1).[1]

Whereas the sign and general behavior (e.g., SBN input was zero during fixation) of each premotor neuron projection were fixed based on physiological knowledge (Langer et al. 1986; Scudder and Fuchs 1992; Scudder et al. 2002) its weight was optimized. This optimization was performed on a data set of conjugate eye movements that included *1*) fixation (−30 to +30° in 5° increments); *2*) sinusoidal smooth pursuit (0.5 Hz, 40°/s peak velocity); *3*) passive sinusoidal whole body rotation with an earth-fixed target (0.5 Hz, 40°/s peak velocity); *4*) passive sinusoidal whole body rotation with a head-fixed target (0.5 Hz, 40°/s peak velocity); and *5*) saccades (amplitudes 3–20°). Each paradigm provided 2,000 data points to the algorithm. Optimization using a rich data set of conjugate eye movements was important to set realistic weights that account for the relative contributions of each neuron type across various oculomotor behaviors (Cullen and McCrea 1993; Cullen et al. 1993b; Hazel et al. 2002; Roy and Cullen 2002). Weights (w_i) for all premotor neuron types ($n = 8$) were obtained using a least-square optimization procedure

$$\overline{FR}(t)_{ABN} = w_1\overline{FR}(t)_{EH\_contra} + w_2\overline{FR}(t)_{PVP\_contra} + \cdots + w_8\overline{FR}(t)_{EH\_ipsi}$$

When freely estimated, the weight of ipsilateral burst-tonic neurons became unrealistically large, whereas the other weights were generally reduced to negligible values (Supplemental Fig. S1*A*, rightmost endpoints). This is not surprising given that burst-tonic and abducens neurons have highly similar discharge patterns across oculomotor behaviors (Sylvestre et al. 2003). To estimate more physiologically realistic values, the weight of ipsilateral burst tonic neurons (BTs) was fixed to different values <0.8 (the weight obtained when freely estimated) and the remaining weights were estimated. All weight values obtained using this approach showed dependence on the ipsilateral BT weight. Notably, all weight sets yielded relatively similar goodness-of-fits ($0.93 \leq VAF \leq 0.96$, measured simultaneously over all five paradigms) to reconstructed ABN discharges (Supplemental Fig. S1*B*).

To determine the "optimal" weight set, the weight values estimated on the conjugate data set were used to predict the discharges of ABNs on a data set of disconjugate saccades that were not used to estimate the weights. The "optimal" weight set was defined as the weight set that accounted for most of the variance in the average ABN firing rates during disconjugate saccades [both converging and diverging disconjugate saccades when both eyes were moving in the neuron's "ON" (i.e., ipsilateral) direction used in the simulations]. Note that for disconjugate saccades, coefficients were taken from this and prior studies when possible (i.e., Sylvestre and Cullen 2002; Sylvestre et al. 2003) and inferred for contra position-vestibular-pause (PVP) neurons based on published data (sensitivities and bias taken from McConville et al. 1994; Roy and Cullen 2002) since most PVPs ramp up during contra saccades without a burst or pause. For neurons that were conjugate and/or for which only conjugate estimations have been done (e.g., eye head neurons), the coefficients of each eye are equivalent to the conjugate estimate/2 (by definition).

RESULTS

The primary goal of this study was to determine whether the modulation of SBNs could account for the increased vergence velocities during disconjugate saccades. The approach chosen to address this problem was twofold and involved *1*) a comprehensive analysis of the timing and dynamic properties of SBNs' discharges during disconjugate saccades and *2*) a quantitative simulation of the command generated by brain stem premotor neurons during conjugate versus disconjugate saccades.

Excitatory burst neurons (EBNs; $n = 30$) and inhibitory burst neurons (IBNs; $n = 44$) were recorded in the paramedian pontine reticular formation (PPRF). The neurons in this study were further categorized as short- or long-lead neurons depending on whether the mean period between the onset of the first spike and the onset of eye velocity was ≤15 or >15 ms, respectively (Cullen and Guitton 1997; Scudder et al. 1988). Comparable numbers of short- and long-lead EBNs ($n = 16$ and 14, respectively) and IBNs ($n = 23$ and 21, respectively) were recorded. A thorough comparison of short- and long-lead EBNs and IBNs was completed for each aspect of the study. Where no differences were found between the discharge patterns of short- and long-lead IBNs and EBNs (with the obvious

[1] The online version of this article contains supplemental data.

exception of the burst lead times), the two populations are discussed as a pooled population.

SBN discharge timing is appropriate to facilitate vergence movements

An example of a short-lead IBN is shown in Figs. 2 and 3. This neuron was typical in that it discharged a compact burst of action potentials during ipsilaterally directed conjugate saccades. Although no action potentials were observed during saccade-free vergence (Fig. 2*A*), the example neuron was active during the saccade component of the disconjugate saccades (Fig. 3*A*). Importantly, no action potentials were observed before or following this interval, despite the presence of a significant but much slower vergence velocity (gray shaded areas in Fig. 3*A*). Figure 3*B* illustrates the relationship between burst duration and saccade duration for this example burst neuron during conjugate saccades and disconjugate saccades (gray and black filled circles, respectively). Burst duration was well related with saccade duration during both conjugate (mean $R^2 = 0.89$, range 0.4–1.00) and disconjugate (mean $R^2 = 0.89$, range 0.46–1.00) saccades. In contrast, burst duration was less correlated ($P < 0.05$) with the total duration of the vergence movement during disconjugate saccades (Fig. 3*C*, mean $R^2 = 0.48$, range 0.03–0.93), where total vergence duration included the combined duration of both the saccade and any slow vergence movement that preceded or followed it. Similar findings were obtained for the analysis of OPNs during the same paradigms (Fig. 2*B*). Implications of these results are further considered in the DISCUSSION.

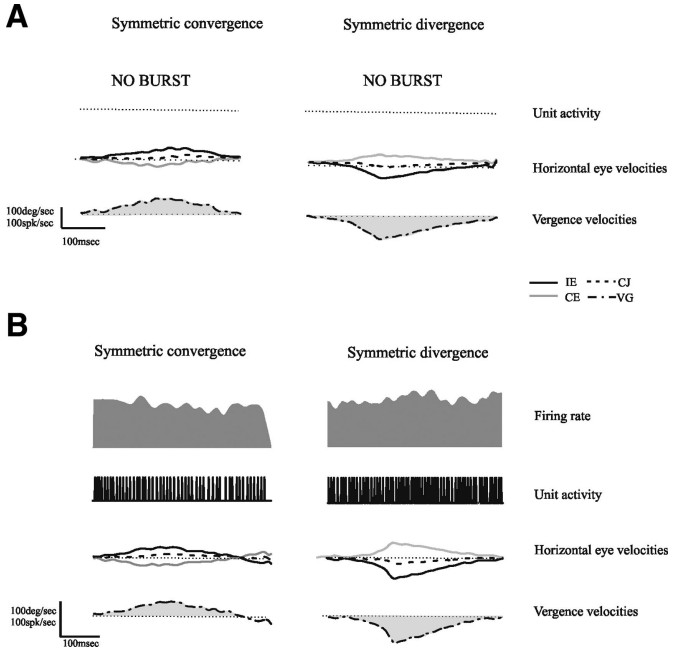

FIG. 2. Example neural activity for a short-lead inhibitory burst neuron (IBN, *A*) and omnipause neuron (OPN) (*B*) during smooth saccade-free vergence. The BN did not fire any action potentials (i.e., firing rate and unit activity are zero) during saccade-free vergence and the OPN did not pause during slow saccade-free vergence. The gray shaded areas in the *top rows* represent the firing rate of the neuron and the unit activity is shown in the *2nd rows*. Also shown are the conjugate (CJ) and vergence (VG) velocity traces as well as the velocity traces of each eye [i.e., the eye ipsilateral (IE) and contralateral (CE) to the recording site]. The light gray shaded areas in vergence velocity traces in *A* and *B* highlight the areas of smooth saccade-free vergence. Horizontal dotted lines denote zero velocity.

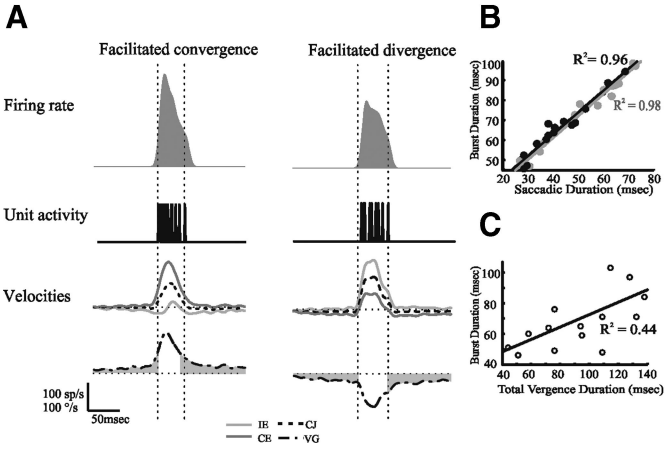

FIG. 3. Example neural activity for a short-lead IBN (*A*) during facilitated vergence. Converging saccades are on the *left* and diverging saccades are on the *right*. The gray shaded areas in the *top row* represent the firing rate of the neuron and the unit activity is shown in the *2nd row*. Also shown are ipsilateral eye (IE) in light gray, contralateral eye (CE) in dark gray, and conjugate (CJ) velocity traces and vergence (VG) velocity traces (*bottom row*) in black. The light gray shaded areas in the vergence velocity traces in *A* highlight the areas of smooth saccade-free vergence. The example IBN (*A*) did not fire any action potentials (i.e., firing rate and unit activity are zero) during saccade-free vergence but started firing at the onset of the saccade. The onset and offset of the saccade were determined using a typical 20°/s velocity criterion, which is marked by vertical dotted lines. Horizontal dotted lines denote zero velocity. *B*: the relationship between the burst duration of a typical IBN and saccade duration in conjugate saccades (gray dots, $R^2 = 0.98$) and in disconjugate saccades immediately preceded by a period of slow vergence (>10 ms; see also Busettini and Mays 2005a) (black dots, $R^2 = 0.96$). *C*: the burst duration, of the same IBN shown in *A*, and total vergence duration (including the saccade-free vergence) ($R^2 = 0.44$).

Testing the null hypothesis: SBNs encode only conjugate eye movement dynamics

The timing of SBNs discharge is coincident with the facilitation of vergence movements during disconjugate saccades. We next quantitatively characterized the signals that are dynamically encoded by the brain stem saccadic burst generator during conjugate and disconjugate saccades using the following approach: First, we used systems identification techniques to provide a movement-based description of the discharge dynamics of each neuron during ipsilaterally directed conjugate saccades. Second, we assessed whether we could predict the discharge of the same neuron during disconjugate saccades based on its responses during conjugate saccades. Third, we directly estimated the sensitivity of individual neurons to the movements of the right/left eyes or the conjugate/vergence profiles on the same data set of disconjugate saccades (see METHODS). Based on their ocular preference during disconjugate saccades, neurons were sorted into five categories (see Table 1). Finally, to fully assess the premotor drive to the extraocular motoneurons during saccades we also characterized SBN activity during OFF-direction saccades (i.e., contralaterally directed saccades).

The original analysis of Cullen and Guitton (1997) provided the simplest firing rate model that can be used to describe the discharge properties of IBNs during conjugate saccades, expressed as

$$FR(t - t_d) = b + r\,\dot{CJ}(t) \quad \text{(Conjugate-est model)} \qquad (3)$$

where FR is the instantaneous firing rate, b is the estimated bias and r is the estimated velocity sensitivity, $\dot{CJ}(t)$ is the velocity of the eye during conjugate saccades, and t_d is the neuron's dynamic lead time. Here this finding was confirmed for IBNs and extended to EBNs (see Supplemental Table S2 for population averages of parameters and VAFs, t_d = 14.1 ± 3.8 and 13.8 ± 2.8 ms, EBNs and IBNs, respectively). Figure 4 shows model fits for a representative EBN and IBN during two conjugate saccades (*top row*; VAF = 0.57 ± 0.16 and 0.57 ± 0.16, EBNs and IBNs; notably VAF values indicated here, and for the subsequent figures, were calculated when fitting the entire data set and not only the example movements that are shown in the figures). Adding an eye position or acceleration term (Fig. 4, *second row*, thick black and gray lines, respectively) to *Eq. 3* did not appreciably improve the model fits (EBNs, VAF = 0.59 ± 0.15 and 0.57 ± 0.15; IBN, VAF = 0.59 ± 0.13 and 0.58 ± 0.13; position and acceleration terms, respectively). Indeed, the position and acceleration parameter values did not differ from zero across neuron types (P = 0.40, P = 0.38, respectively, one-way ANOVA; see METHODS).

REJECTING THE NULL HYPOTHESIS: THE CONJUGATE PREDICTION FAILS. The discharge dynamics of the EBNs and IBNs were next analyzed during disconjugate saccades. For each neuron, we first determined whether the simple model estimated earlier during conjugate saccades (*Eq. 3*) could predict its activity during disconjugate saccades. Figure 5 shows the activity of an example short-lead EBN during converging versus diverging disconjugate saccades (i.e., Fig. 5, *A* and *B*, respectively) elicited during "monocular" saccades (i.e., Müller paradigm; see METHODS). Note the large differences in dynamics for the two eyes during these movements: in the converging case (Fig. 5*A*) the contralateral eye moved, whereas the ipsilateral eye was relatively stationary; in the diverging case (Fig. 5*B*) the ipsilateral eye moved, whereas the contralateral eye was relatively stationary. Notably, the conjugate component of the

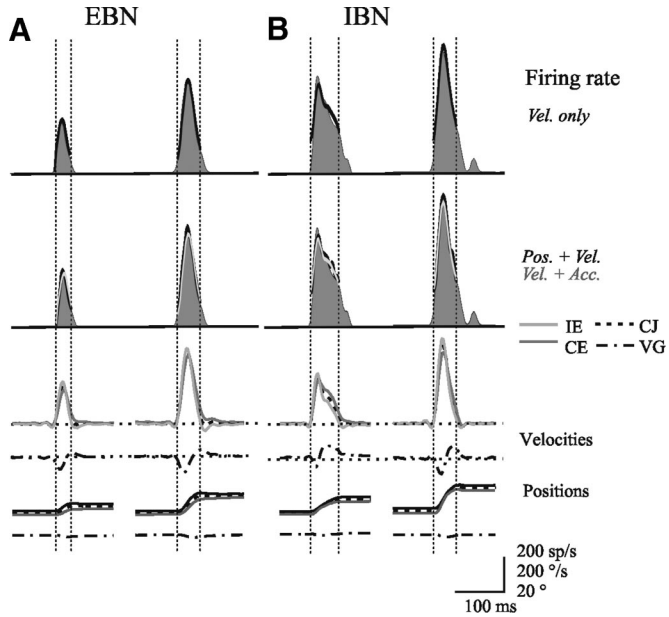

FIG. 4. Example discharges from a short-lead excitatory burst neuron (EBN, *A*) and IBN (*B*) during 2 conjugate saccades. The *top row* represents the neurons' firing rates (gray shaded areas) and the model fits (thick black curve) obtained with *Eq. 3*. The *2nd row* shows the same firing rate traces duplicated for clarity, but with the model fits obtained using *Eq. 3* + eye position (thick black curve) and *Eq. 3* + eye acceleration (thick gray curve). Also shown are ipsilateral eye (IE), contralateral eye (CE), and conjugate (CJ) velocity traces (*3rd row*) and position traces (*5th row*), and vergence (VG) velocity traces (*4th row*) and position traces (*bottom row*). Vertical dotted lines denote saccade onsets and offsets; horizontal dotted lines represent zero velocity.

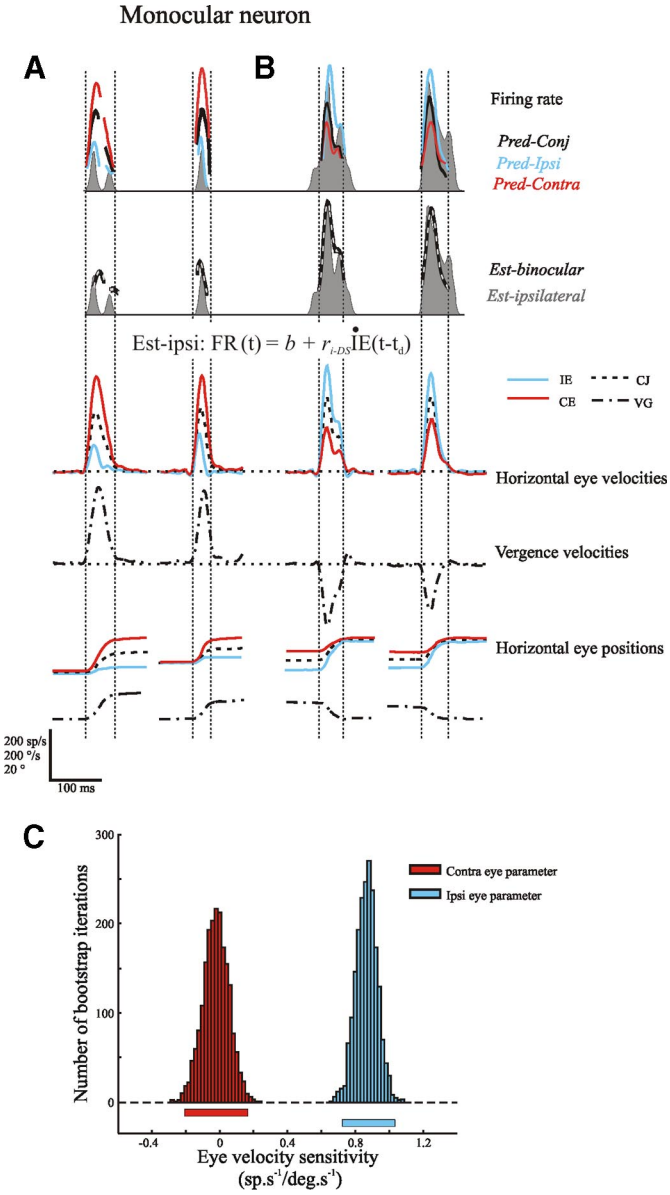

FIG. 5. Example discharges from an example monocular short-lead EBN (same neuron as in Fig. 3*A*) during (*A*) converging disconjugate saccades (contralateral eye moves more) and (*B*) diverging disconjugate saccades (ipsilateral eye moves more). The *2nd row* shows the same firing rate traces duplicated for clarity. Predicted model fits using *Eq. 3* and conjugate, ipsilateral, and contralateral eye velocities are shown in the *top row* in black, blue, and red, respectively. Note the poor fits obtained when the conjugate and contralateral parameters are used to predict the firing rate of this neuron compared with the prediction using the ipsilateral eye (*top row*, *red* and *black traces* compared with *blue trace*). Estimated model fits using the binocular model (*Eq. 4*) are shown in the *2nd row* (thick black curve). Estimated model fits using the reduced ipsilateral model (equation below the firing rate traces) are also shown (dashed gray curve). *C*: bootstrap histograms and 95% confidence intervals (thick horizontal bars) for this neuron. Note the 95% confidence interval for the contralateral eye (red bar) overlaps with zero.

movements was comparable in the two conditions. For the example neuron, as well as the majority of SBNs (54%) in our study, the conjugate-based prediction tended to overshoot the firing rate when the preferred eye moved less (i.e., during the diverging movements for this example neuron, Fig. 5*A*) and to undershoot when the preferred eye moved more (Fig. 5*B*). Specifically, this neuron's activity was best predicted when ipsilateral (superimposed blue trace; $VAF_{pred\text{-}ipsi} = 0.62$) rather than conjugate or contralateral eye velocities (superimposed black and red traces; $VAF_{pred\text{-}conj} = 0.49$ and $VAF_{pred\text{-}contra} = 0.13$) were the model inputs.

The results of the prediction-based analysis suggest that the majority of the neurons preferentially encode the movement of one eye rather than the conjugate eye velocity. We next investigated whether estimating a more complex model—a binocular expansion of the conjugate model (*Eq. 3*)—might provide an improved description of neuronal discharges during disconjugate saccades

$$FR(t - t_d) = b + r_i \dot{IE}(t) + r_c \dot{CE}(t) \quad \text{(Binocular-est model)} \quad (4)$$

where b, r_i, and r_c are the bias and ipsilateral and contralateral eye velocity sensitivities of the neuron, respectively (subscripts i and c refer to the ipsilateral and contralateral eyes relative to the recording site, respectively), and $\dot{IE}(t)$ and $\dot{CE}(t)$ are instantaneous ipsilateral and contralateral eye velocities, respectively. For each parameter in *Eq. 4*, bootstrap 95% confidence intervals were used to reduce the model to its simplest form.

When the parameters of *Eq. 4* were freely estimated, a very good description of the example EBN's discharge patterns was obtained (Fig. 5, $VAF_{est\text{-}bino} = 0.78$, *second row*, thick black curve). The 95% bootstrap confidence intervals revealed that only the ipsilateral eye velocity sensitivity term (r_i) and bias were significantly different from zero (Fig. 5*C*). Thus removing the contralateral eye velocity sensitivity term (r_c) from *Eq. 4* had a negligible impact on our ability to fit this neuron's discharge (gray curve, *second row*, Fig. 5; $VAF_{est\text{-}bino} = 0.78$, $VAF_{est\text{-}ipsi} = 0.77$, $\Delta BIC = 0$). We therefore conclude that this neuron is monocular with a preference for the ipsilateral eye. Overall, we found that most SBNs (>70%) preferentially encoded the velocity of an individual eye (average bias and ipsilateral and contralateral eye velocity sensitivities of the SBNs were 150 ± 58, 0.32 ± 0.28, and 0.43 ± 0.30).

Notably, a minority of the SBNs in our population had no monocular tuning. Figure 6 shows the discharge patterns of such an example "conjugate" SBN during disconjugate saccades. The neural activity of this neuron was best predicted when conjugate (Fig. 6, superimposed black trace, $VAF_{pred\text{-}conj} = 0.71$) rather than ipsilateral or contralateral eye velocities (superimposed blue and red traces; $VAF_{pred\text{-}ipsi} = 0.5$ and $VAF_{pred\text{-}contra} = 0.41$) were the model inputs. The goodness-of-fit provided by the conjugate prediction was nearly as good as that provided by *Eq. 4* when its parameters were freely estimated ($VAF_{pred\text{-}conj} = 0.71$ vs. $VAF_{est\text{-}bino} = 0.73$). Furthermore, the estimated ipsilateral and contralateral eye velocity sensitivities of this neuron were statistically identical (Fig. 6*C*). Since, by definition, a neuron that has equal sensitivities to both eyes' movements has no vergence sensitivity (recall, vergence = left eye − right eye), this neuron similarly encoded conjugate eye movement

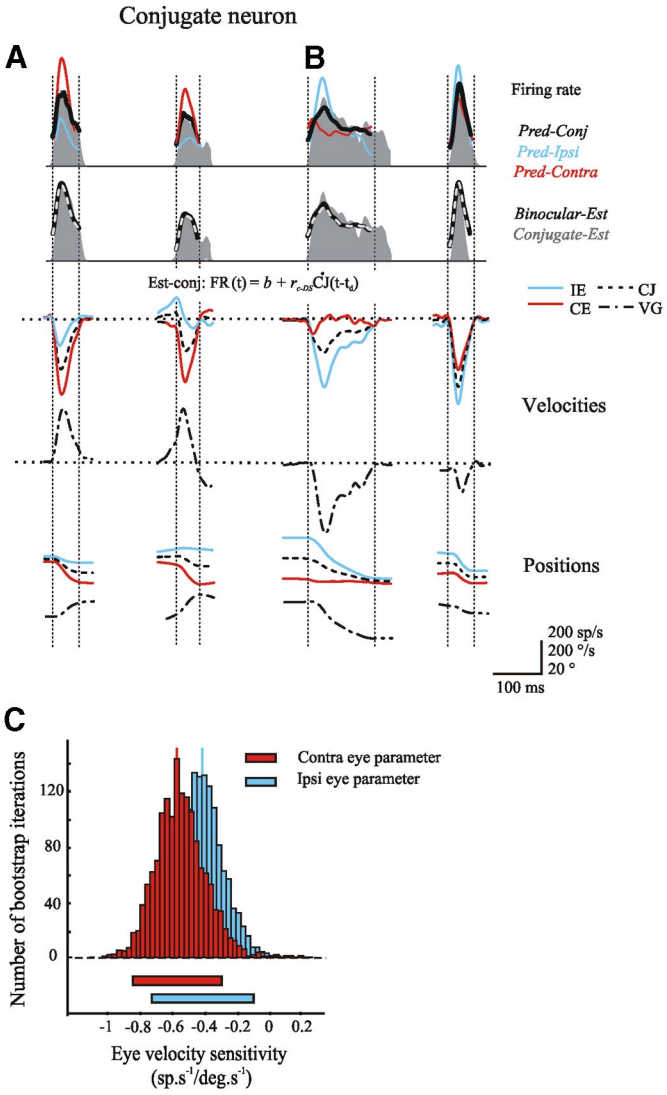

FIG. 6. Example discharges from an example conjugate short-lead IBN during (*A*) converging disconjugate saccades [contralateral eye (CE) moves more] and (*B*) diverging disconjugate saccades [ipsilateral eye (IE) moves more]. Note the good fits obtained when the conjugate parameters are used to predict the firing rate of this neuron (*black trace* on firing rate) compared with when the ipsilateral and contralateral eye velocity are used (*blue* and *red traces* respectively, superimposed on firing rate). The *2nd row* shows the same firing rate traces (duplicated for clarity) and the estimated model fits using the binocular model (*Eq. 2*, thick black curve). Estimated model fits using the reduced conjugate model (equation below the firing rate traces) are also shown (dashed gray curve). *C*: bootstrap histograms and 95% confidence intervals (thick horizontal bars) for this neuron.

dynamics during both conjugate and disconjugate saccades. Thus as expected, when the r_i and r_c parameters in *Eq. 4* were replaced by a conjugate velocity sensitivity, the obtained model fit was nearly the same as that obtained with the full binocular model (Fig. 6, *second panel*, gray curve, $VAF_{est\text{-}bino} = 0.73$, $VAF_{est\text{-}conj} = 0.71$; $\Delta BIC = 0$).

For each EBN and IBN, a $Ratio_{dyn}$ index was computed based on the estimated parameters of *Eq. 4* (see METHODS) to objectively assign each neuron to one of five ocular categories (Table 1). The distributions of $Ratio_{dyn}$ obtained using this method for EBNs and IBNs are shown in Fig. 7, *A* and *B*. Comparisons of the results of our prediction and estimation-

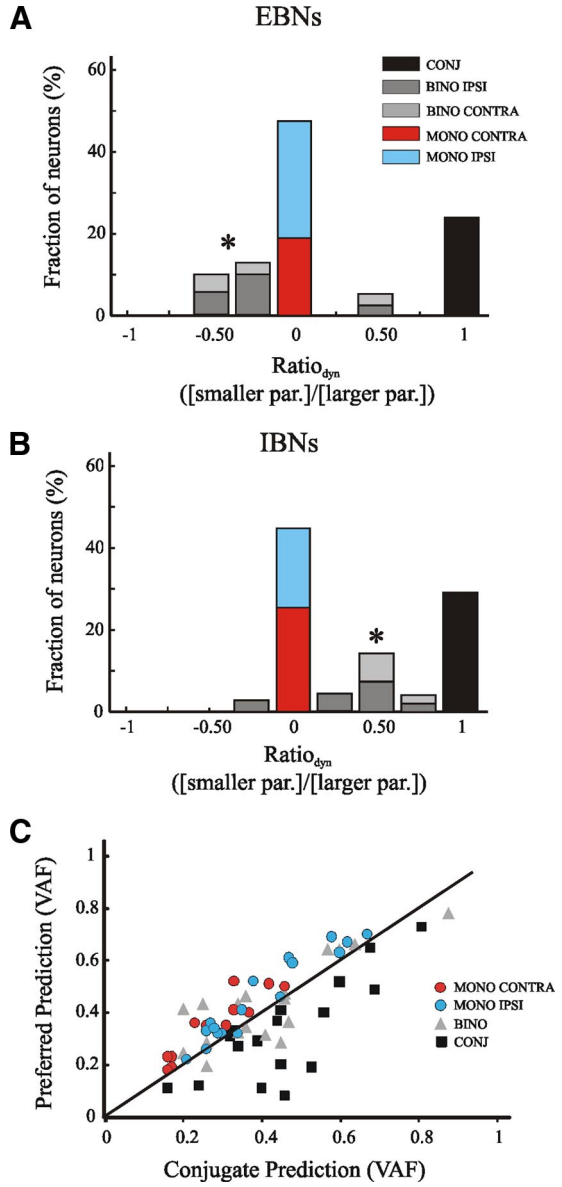

FIG. 7. Distribution of Ratio$_{Dyn}$ indexes for EBNs (*A*) and IBNs (*B*). Columns marked with an asterisk indicate a greater number of binocular EBNs with a negative Ratio$_{dyn}$ (*A*) and a greater number of IBNs with a positive Ratio$_{dyn}$ (*B*). *C*: comparison of the results of the prediction and estimation-based analyses. Each symbol represents an individual neuron. The firing rates of neurons that were classified as monocular, based on their Ratio$_{dyn}$ value, were best predicted when the preferred eye velocity was the input (red and blue circles), whereas the firing rates of neurons that were classified as conjugate were better predicted when conjugate eye velocity was the input to the model.

based analyses are shown in Fig. 7*C*. Each symbol represents an individual neuron. The firing rates of neurons that were classified as monocular based on their *Ratio$_{dyn}$* value were best predicted when the preferred eye velocity was the input (i.e., red and blue circles above the line of unity in Fig. 7*C*), whereas the firing rates of neurons that were classified as conjugate were better predicted when conjugate eye velocity was the input to the model (black squares below the line of unity in Fig. 7*C*). The average VAFs and difference in BIC provided by the complete binocular versus reduced models are summarized for each of the five categories of neurons in Table 2.

The above-cited findings were confirmed when the analysis of our samples of EBNs and IBNs was performed again using the following model

$$FR(t - t_d) = b + r_{cj}\,\dot{CJ}(t) + r_{vg}\,\dot{VG}(t) \quad \text{(Vergence-est model)} \quad (5)$$

where $\dot{CJ}(t)$ and $\dot{VG}(t)$ are instantaneous conjugate and vergence velocities, respectively. We found that 75% of EBNs and 70% of IBNs encode significant vergence velocity sensitivities (r_{vg}) during disconjugate saccades. Moreover, both *Eq. 4* and *Eq. 5* yielded similar conclusions on a neuron-by-neuron basis.

COMPARISON ACROSS NEURON TYPES. Statistical analyses were performed to compare the discharge properties of short- and long-lead EBNs and IBNs. During conjugate and disconjugate saccades, most parameters evaluated were statistically identical across all neuron types ($P > 0.05$, with the exception that biases were slightly less for short-lead EBNs than for long-lead IBNs). Although the distributions of long- and short-lead EBNs and IBNs across the five categories of ocular preference were not identical, the differences were highly nonsignificant ($P = 0.98$; χ^2 test on a 4×5 contingency table; see METHODS). Moreover, for the metric-based analyses, there were no significant differences in the distribution of the four neuron types across the five categories of ocular preference ($P = 0.36$ and 0.76, NOS and peak analyses, respectively; χ^2 test on a 4×5 contingency table). Thus except for the prelude discharges of long-lead neurons, all four neuron types tested had similar discharge properties during both conjugate and disconjugate saccades.

CALCULATION OF THE NET PREMOTOR DRIVE. The activity of SBNs was also characterized during OFF-direction (i.e., contralaterally directed) saccades to fully assess the premotor drive to the extraocular motoneurons. Overall, we found that the OFF-direction discharges were relatively minor during both conjugate and disconjugate saccades and thus had only a negligible impact on eye velocity. During conjugate saccades, the majority of EBNs (26/30) were completely silent, whereas the remaining 4 neurons had very small bursts that were poorly related to saccade dynamics (mean VAF = 0.22 ± 0.06; Supplemental Table S2). Similarly, during disconjugate saccades, the same EBNs, as well as 2 additional EBNs, produced minor responses (mean VAF = 0.20 ± 0.06). The majority of IBNs were also silent (30/44) and the remaining neurons produced a few spikes during OFF-direction conjugate (n = 14/44; Supplemental Table S1) and disconjugate (n = 16/44; Supplemental Table S2) saccades.

METRIC ANALYSIS OF CONJUGATE AND DISCONJUGATE SACCADES. To compare our sample of EBNs and IBNs with those previously described in the literature (Cullen and Guitton 1997; Kaneko et al. 1981; Scudder 1988; Strassman et al. 1986a,b; Yoshida et al. 1982), saccade-related burst activity was also characterized using classical metric-based analyses. During conjugate saccades, the number of spikes in a neuron's saccadic burst (NOS) was linearly related to the conjugate amplitude (ΔCJ) of the eye movement (NOS = $b + z\Delta CJ$; see Supplemental Table S2). In addition, the peak saccadic firing rates of neurons were also linearly correlated to peak conjugate velocity, although this relationship was generally more noisy ($FR_{\max} = b + p\,CJ_{\max}$; see Supplemental Table S2).

TABLE 2. *Summary of model predictions and estimations during disconjugate saccades*

	$VAF_{pred\text{-}conj}$	$VAF_{pred\text{-}pref}$	$VAF_{est\text{-}bino}$	$VAF_{est\text{-}red}$	ΔBIC
MONO-Ipsi	0.39 ± 0.15	0.44 ± 0.16	0.48 ± 0.15	0.47 ± 0.15	0.01 ± 0.02
MONO-Contra	0.28 ± 0.10	0.35 ± 0.11	0.43 ± 0.09	0.42 ± 0.08	0.02 ± 0.02
CONJ	0.46 ± 0.17	0.46 ± 0.17	0.51 ± 0.18	0.51 ± 0.06	0.01 ± 0.01
BINO-Ipsi	0.47 ± 0.21	0.42 ± 0.14	0.52 ± 0.17	0.36 ± 0.19	0.30 ± 0.01
BINO-Contra	0.44 ± 0.10	0.40 ± 0.24	0.59 ± 0.08	0.50 ± 0.17	0.21 ± 0.08

Values are means ± SD. VAF, variance-accounted-for; BIC, Bayesian Information Criteria; $VAF_{pred\text{-}conj}$, the VAF when predicting the firing rate using the conjugate velocity; $VAF_{pred\text{-}pref}$, the VAF when predicting the firing rate using the preferred eye velocity; $VAF_{est\text{-}bino}$, the VAF when estimating using both eyes; $VAF_{est\text{-}red}$, the VAF when estimating using the preferred eye (i.e., conj, ipsi, or contra); ΔBIC, BIC binocular model − BIC reduced model.

During disconjugate saccades, this approach was modified to account for the movements of both eyes (see *Eqs. 1* and *2* in METHODS).

The parameter values estimated with these models were then used to compute $Ratio_{NOS}$ and $Ratio_{FRmax}$ indices (see METHODS) that were used to objectively assign each neuron to one of the five categories (Table 1). The distributions of $Ratio_{NOS}$ and $Ratio_{FRmax}$ indexes are shown in Fig. 8 (*left* and *right*, respectively) for EBNs and IBNs (Fig. 8, *A* and *B*, respectively). The two analysis approaches yielded similar population results for both types of neurons. In general, most EBNs and IBNs were monocular (blue and red bars).

These results can be directly compared with those of Zhou and King (1998), who performed the only other characterization of EBN discharge during disconjugate saccades using a NOS-based approach identical to that shown in *Eq. 1*. For each neuron in their sample, Zhou and King computed an ocular index (OI), which can be converted to a Ratio index to facilitate comparison (see METHODS). The distribution of $Ratio_{NOS}$ indexes that was estimated from Zhou and King (1998) using this approach is shown in Fig. 8*A* (*inset*, *top left*). No significant differences in the distribution of neurons across the five categories of ocular preference (Table 1) were observed between the two studies ($P = 0.53$; χ^2 test on a 2 × 5 contingency table).

COMPARISON OF DYNAMIC AND METRIC ANALYSES. It is important to note that on a neuron-by-neuron basis, similar conclusions were obtained using both the dynamic and NOS-based metric analyses (refer to Fig. 5 for dynamic analysis results). Overall, 61% of the neurons were classified in the same category of ocular preference (Table 1) using both dynamic and metric analyses. In the DISCUSSION, we consider the limitations of the metric-based approach, which does not take advantage of the information encoded in the temporal pattern of action potentials.

Can the brain stem saccade generator provide the vergence drive required to drive the abducens motoneurons during disconjugate saccades?

SIMULATION DESIGN. A computer-based simulation was implemented (see METHODS) in which the discharges of sac-

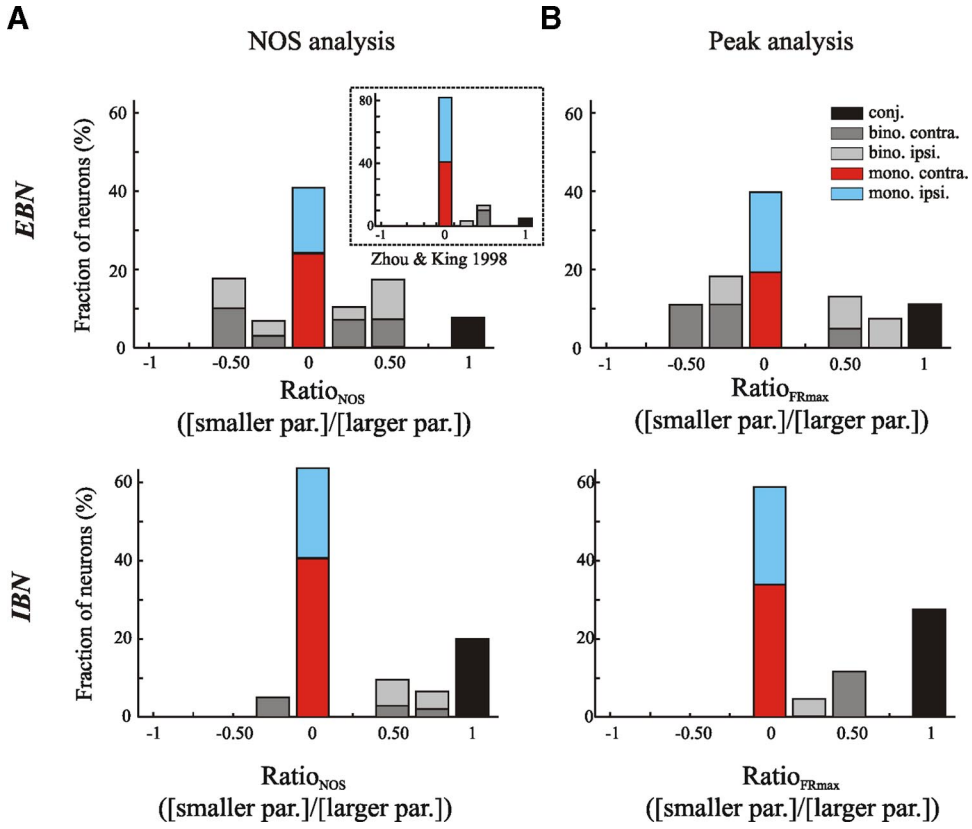

FIG. 8. Distribution of $Ratio_{NOS}$ indexes (*A*) and $Ratio_{FRmax}$ indexes (*B*) for EBNs (*top row*) and IBNs (*bottom row*). *Inset*: distribution of $Ratio_{NOS}$ for the sample of EBNs in Zhou and King (1998), estimated from their Fig. 3*B*.

cadic burst neurons (present study) were combined with those of other saccade-related premotor neurons (previous studies; see Supplemental Table S1) with known projections to the ABN. This allowed us to determine whether the SBNs encode sufficient information to shape motoneuron discharge during both disconjugate and conjugate saccades, or whether premotor input from a separate vergence subsystem (see DISCUSSION of Busettini and Mays 2005b) is needed. The sign of projection for each premotor neuron was fixed based on physiological knowledge (Langer et al. 1986; Scudder and Fuchs 1992; Scudder et al. 2002) and their weights were optimized. Importantly, pure vergence-related inputs (e.g., from vergence-velocity neurons) were deliberately omitted from the simulation. Example reconstructed average population drives during a conjugate saccade are shown in Fig. 9.

PREDICTION DURING DISCONJUGATE SACCADES. The weight values estimated on the conjugate data set (Supplemental Fig. S1) were used to predict the discharge of ABNs on a data set of disconjugate saccades (i.e., a data set different from that originally used to estimate the weights). The "optimal" weight set (defined as the weight set that yielded the largest VAF during the prediction) accounted for 98% of the variance contained in average ABN firing rates during disconjugate saccades (Fig. 10*A*). As is shown in Fig. 10*B*, the goodness-of-fit for the prediction was equivalent to that obtained when the weights were estimated during conjugate saccades. Notably, this general result held for all weight sets (i.e., irrespective of whether the BT weight was set relatively small or large). Thus this result supports the proposal that additional vergence-related premotor signals are not required to shape the activity of abducens motoneurons.

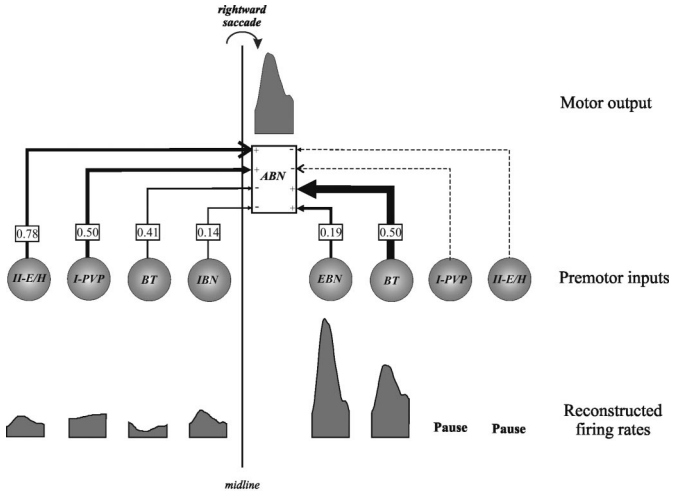

FIG. 9. Schema of the circuitry used for simulations. Eight premotor neuron types were selected, 4 from the ipsilateral brain stem and 4 from the contralateral brain stem. The nature of each connection is indicated in the box labeled abducens nucleus (ABN) as (+) for excitatory connections or (−) for inhibitory connections. The shading of neurons' cell bodies indicates whether they increase (dark gray) or decrease (light gray) their discharges for a rightward saccade. "Optimal" weights are superimposed on each connection. The thickness of arrows indicates the relative contribution of each neuron type during saccades, using the weights shown. Reconstructed population discharges are shown for each neuron type during an example conjugate saccade (*bottom row*, gray shaded areas). Weights were optimized on a conjugate data set that included *1*) fixation (−30 to +30° in 5° increments), *2*) sinusoidal smooth pursuit (0.5 Hz, 40°/s peak velocity); *3*) passive sinusoidal whole body rotation with an earth-fixed target (0.5 Hz, 40°/s peak velocity); *4*) passive sinusoidal whole body rotation with a head-fixed target (0.5 Hz, 40°/s peak velocity); and *5*) saccades (amplitudes 3–20°). Each paradigm provided 2,000 data points to the algorithm.

ANALYSIS OF SIMULATION WEIGHTS. The weight sets were analyzed based on the contribution of each neuron type in shaping ABN discharges (where we define contribution $= w_i \times [\int \overline{FR}_i(t)/\int \overline{CJ}_{ABN}(t)]$, where "$i$" represents one of eight premotor neuron types). Figure 10*C* plots the contribution of the eight premotor neuron types as a function of the weight of ipsilateral BT neurons during saccades.

Two main observations can be made from the "optimal" weight set. First, the estimated weights of ipsilateral EBNs and contralateral IBNs were approximately the same. This is consistent with both neuron types projecting with similar densities to the ABN (Strassman et al. 1986a,b) and with IBNs inhibiting most (>80%) contralateral ABNs during ipsilateral saccades (Sylvestre and Cullen 1999). Second, additional excitatory drives to the ABN during saccades originate from ipsilateral burst tonic neurons (BTs) and from contralateral eye–head neurons (EHs) and type I position-vestibular-pause neurons (PVPs). In addition, as expected, contralateral BTs and IBNs and ipsilateral EHs and PVPs provide inhibitory inputs to ABN motoneurons during saccades. Note that EHs and PVPs provide equal excitatory contributions, which are half that provided by BTs. This ratio is consistent with that previously deduced to predict ABN discharges during conjugate smooth pursuit, VOR in the dark, and cancellation of the VOR (Cullen et al. 1993b).

DISCUSSION

The present results conclusively demonstrate that *1*) the brain stem saccadic generator, which is commonly assumed to drive only the conjugate component of eye movements, carries substantial vergence-related information that is temporally and dynamically related to the dynamics of disconjugate saccades; and *2*) the resulting premotor command is, in fact, sufficient to drive the agonist extraocular motoneurons during disconjugate saccades. Thus the premotor command to generate diverging saccades is present in what had been mistakenly assumed was the "conjugate" saccade generator. Overall, our experimental and theoretical results strongly support the hypothesis that the brain stem saccadic circuitry shapes the activity of ABN neurons by encoding integrated conjugate and vergence premotor commands (Cova and Galiana 1996; King and Zhou 2000, 2002; Sylvestre et al. 2003).

Comparison with previous reports: conjugate saccades

The responses of SBNs during conjugate saccades, first characterized using traditional metric-based approaches, and results highly comparable to those that have been previously described were obtained (Cullen and Guitton 1997; Hepp and Henn 1983; Keller 1974; Luschei and Fuchs 1972; Scudder 1988; Strassman et al. 1986a,b; Van Gisbergen et al. 1981). Next, an analysis of the dynamic relationship between the IBN discharges and eye velocity yielded results equivalent to those of prior studies (Cullen and Guitton 1997). Finally, we found that EBNs encode saccade dynamics during conjugate saccades with the same accuracy as do

IBNs. This latter finding confirms the proposal that EBNs, like IBNs, encode saccade trajectories in their spike trains (Eckmiller et al. 1980; Hepp and Henn 1983; Robinson 1973; Van Gisbergen et al. 1981).

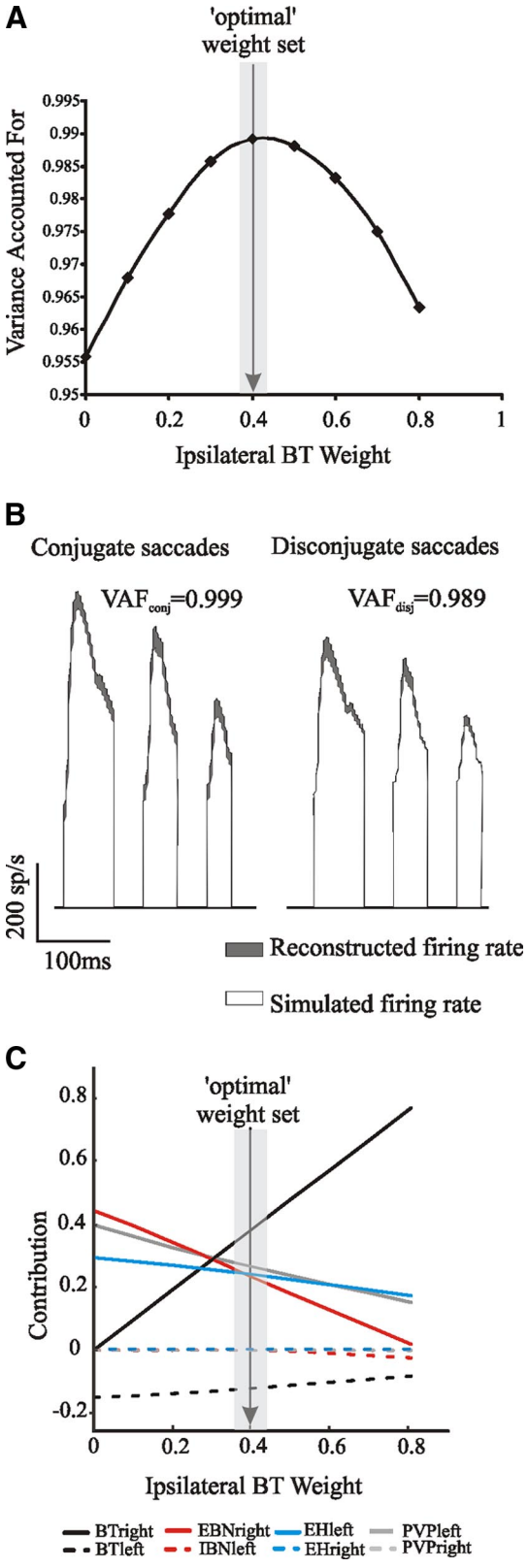

Timing and dynamics of SBN burst activity are appropriate to facilitate vergence during disconjugate saccades

Although numerous studies have shown that the timing of SBN bursts is appropriate to drive conjugate saccades, this study is the first to have systemically evaluated the burst timing during saccade-free slow vergence and disconjugate saccades. During disconjugate saccades burst onsets and durations were tightly linked to saccade onsets and durations, respectively. In contrast, SBNs did not discharge during periods of saccade-free vergence that preceded or followed disconjugate saccades. Since the onset of saccade-facilitated vergence is coincident with saccade onset (Busettini and Mays 2005a), our results show that the premotor drive from the saccadic burst generator is appropriately timed to facilitate vergence velocity during disconjugate saccades. Moreover, these results complement those of Busettini and Mays (2003) showing that the OPN pause is similarly linked to the saccadic component of disconjugate saccades. Taken together these findings provide strong evidence that the vergence facilitation observed during disconjugate saccades occurs only when the saccadic burst generator (i.e., SBNs) is active.

To determine whether SBNs encode similar signals during conjugate and disconjugate saccades, we analyzed neuronal discharges during disconjugate saccades using metric-based and dynamic-based approaches. Only one previous study had evaluated SBNs during disconjugate saccades (Zhou and King 1998). The study used a metric-based approach and its overall conclusion was that the burst activity of EBNs was better correlated with the movement of an individual eye than the conjugate eye movement during disconjugate saccades.

In the present study, results highly comparable to those of Zhou and King (1998) were obtained for both IBNs and EBNs. However, the NOS-based approach is limited because it ignores important information that is encoded within neuronal discharge dynamics (Cullen and Guitton 1997b; Eckmiller and Mackeben 1980; Eckmiller et al. 1980; Hepp and Henn 1983; Robinson 1973; Van Gisbergen et al. 1981). As a result, these findings are consistent with the hypothesis that the premotor saccadic circuitry plays a role in facilitating vergence shifts, but cannot rule out the alternative possibility that the overall contribution of the premotor saccadic circuitry is relatively unimportant compared with that of the vergence subsystem (e.g., see DISCUSSION of Busettini and Mays 2005b). To determine whether SBNs play a significant role in facilitating vergence velocity during disconjugate saccades we used a dynamic-based approach to explicitly describe the relationship between the temporal pattern of neuronal firing and the velocity of each eye. Our results show that vergence-related signals are dynamically encoded in the burst of most SBNs during disconjugate saccades.

FIG. 10. Simulation results. *A*: prediction variances-accounted-for (VAFs) for the data set of disconjugate saccades plotted as a function of the weight of ipsilateral burst tonic neurons (BTs) used to determine the "optimal" weight set. *B*: comparison of ABN firing rates reconstructed using models estimated on the data (gray shaded areas) and using the simulation (white shaded areas) during 3 conjugate (*left*) and 3 disconjugate saccades (*right*). Note that both diverging and converging disconjugate saccades could be fit equally well (0.9975 vs. 0.9805). *C*: contribution of the 8 premotor neuron types to shaping ABN discharges, plotted as a function of the weight of ipsilateral BTs. Positive and negative values indicate excitation and inhibition, respectively.

Role of the saccadic burst generator during saccade–vergence interactions

Several models have been proposed to account for how vergence is facilitated when it is combined with a saccade (Busettini and Mays 2005a; Cova and Galiana 1995, 1996; King and Zhou 2002; Kumar et al. 2006; Mays and Gamlin 1995; Zee et al. 1992). The results of recent behavioral studies, which have shown that saccade dynamics are an important determinant of the dynamics of vergence facilitation, have led to the rejection of the two most influential models: the "Multiply Model" and the "Saccade-Related Vergence Burst Neuron Model" (Busettini and Mays 2005b; Zee et al. 1992; Zhang et al. 1992). Accordingly, to account for the correlation between conjugate and vergence movements, these investigators have proposed that SBNs exclusively encode conjugate saccadic dynamics and that projections from these conjugate SBNs to the vergence premotor pathway underlie the vergence facilitation during disconjugate saccades. Our findings do not support this proposal. First, if the drive from the vergence burst neurons encoded all of the vergence command to drive the vergence part of the saccadic eye movement during disconjugate saccades (i.e., suggested by Busettini and Mays 2005b) this would imply that the SBNs neurons should then code only conjugate eye movements. We do not see this in our data; the results of both the metric-based and dynamic-based approaches demonstrated that SBNs do not solely encode conjugate saccade dynamics. Alternatively, one could consider an intermediate case in which vergence burst neurons encoded half of the vergence command to drive the vergence part of the saccadic eye movement during disconjugate saccades. However, in this scenario our analysis would have estimated larger gains for the preferred eye during disconjugate saccades relative to the gain estimated during conjugate saccades. Again, this was not observed. Indeed, we found that discharge of the majority of neurons during disconjugate saccades could be predicted based on the gains estimated during conjugate saccades (see Fig. 5).

Our computer-based simulations further support the proposal that the vergence-related information encoded by the premotor saccadic circuitry can largely account for vergence facilitation during disconjugate saccades. Notably, motoneuron discharges were well predicted despite the highly conservative assumptions that were made: *1*) weight sets were estimated to reproduce ABN neuron discharges during five different conjugate behaviors (Cullen et al. 1993; Hazel et al. 2002) and were then validated on disconjugate saccades that were not included in the estimation process; and *2*) simulating average population discharges rather than individual neuron discharges restricted the number of weights to optimize, and thus the simulation's flexibility. Moreover, this conclusion was very robust in that it was not sensitive to the specific weight set used (see Fig. 11*A*). Taken together, our results are consistent with a model in which integrated control at the level of the brain stem saccadic burst generator drives saccades in three-dimensional space since the vergence information encoded by this premotor pathway is largely sufficient to drive abducens motoneurons during disconjugate saccades (Fig. 11*A*).

Notably, as shown in Figs. 2 and 3, SBNs are silent during the slow component of disconjugate gaze shifts and pure vergence movements, respectively. Overall, this suggests that although the SBNs function to rapidly drive the eyes to a new position, an additional command (i.e., from premotor neurons that project directly to the ABN) is required to ultimately align the eyes on target. Although no such input has been identified to date, a preliminary report has described neurons encoding slow vergence information near the ABN (Gnadt et al. 1988). Our study was not designed to address whether such an additional input is driven by a shared controller or separate subsystem. Nevertheless, it is likely that both groups of premotor neurons would be under the control of an integrated controller where, for example, the BNs might have a higher threshold for activation (in terms of motor error); such an organization would ensure accurate redirection of the gaze axes.

To model the neural control of horizontal eye movements it is important to also consider the activation of the medial rectus muscle. Lesion studies (Gamlin et al. 1989) and anatomical studies (Highstein and Baker 1978) suggest that the abducens internuclear neurons (AINs) provide a primary input to the medial rectus subdivision of the contralateral oculomotor nucleus for the control of saccades. Both AINs and abducens motoneurons (AMNs) discharge similarly during slow eye

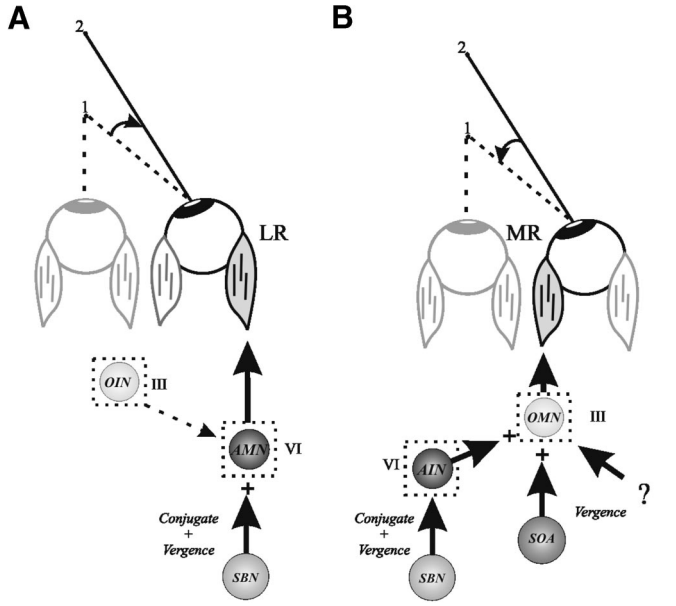

FIG. 11. Neural circuitry involved in generating disconjugate saccades. *A*: when the lateral rectus is the agonist muscle (e.g., during diverging saccades), the SBNs provide the abducens motoneurons with an integrated vergence/conjugate command to drive the movement of the eye. In this framework, the OIN pathway has little influence on the saccades produced by the lateral rectus in the contralateral eye (Gamlin et al. 1989). *B*: framework for the control of disconjugate saccades for the same eye when the medial rectus is the agonist muscle. When the eye moves medially (i.e., during converging saccades), inputs from AINs provide an important input for driving the saccade. However, since abducens motoneurons and abducens internuclear neurons discharge similarly during conjugate and disconjugate saccades, an additional vergence input is required. Consistent with this framework are reports that neurons in the SOA, which project to the oculomotor nucleus, discharge during slow vergence eye movements and discharge at increased rates during disconjugate saccades (Mays et al. 1986; Zhang et al. 1992). For simplicity, the BTs have been excluded from this schematic diagram. Notably, these neurons also have direct inputs to the ABN and also encode vergence-related information (Sylvestre et al. 2003). ABN, abducens nucleus; AIN, abducens internuclear neuron; AMN, abducens motoneuron; III and VI, oculomotor and abducens nuclei; LR and MR, lateral and medial recti; OIN, oculomotor internuclear neuron; OMN, oculomotor motoneuron; SBN, saccadic burst neuron; SOA, supraoculomotor area.

movements and conjugate saccades (Gamlin et al. 1989; Mays and Porter 1984). Moreover, whereas King and Zhou (2002) reported that the majority of AINs had a preference for the contralateral eye during pursuit (note that the method of identification was not explicitly stated), Sylvestre and Cullen (2002) found that AIN and motoneurons appear to have comparable ocular tuning during disconjugate saccades. If AINs and AMNs do have similar discharge patterns, then an additional command would be required at the level of the medial rectus motoneurons (Cova and Galiana 1996; Gamlin et al. 1989; King and Zhou 2002) to appropriately activate the medial rectus muscle.

Inputs from vergence-specific neurons located in the midbrain are likely candidates to provide at least some of this input (Fig. 11*B*); these neurons carry vergence-related information and project to the medial rectus motoneurons in the oculomotor nucleus (e.g., near response neurons) (Mays et al. 1986; Zhang et al. 1992). However, it is unclear whether the discharge from these vergence neurons would be sufficient to account for the saccadic vergence-related activity of the oculomotor motoneurons. For example, it has been hypothesized that the addition of vergence-related signals encode a difference in eye position signals encoded by monocular integrators (i.e., nucleus prepositus or vestibular neurons) that would ultimately reflect a binocular alignment signal (King and Zhou 2002). The predictions from these circuits (Fig. 11, *A* and *B*) are also consistent with clinical studies of internuclear ophthalmoplegia (Leigh and Zee 1999) showing that interruption or inactivation of the INN (internuclear neurons of the abducens nucleus) pathway impairs adductions (i.e., movements controlled by the medial rectus) but preserves abduction.

Source of vergence-related signals

Although the source of the vergence-related signals to SBNs remains unknown, there are several putative sites. Two likely candidates are the central mesencephalic reticular formation (cMRF) and the superior colliculus (SC). Both of these structures receive inputs from disparity-sensitive cortical regions including the frontal eye fields (Ferraina et al. 2000; Gamlin and Yoon 2000) and lateral intraparietal area (Gnadt and Beyer 1998). Furthermore, stimulation of the SC and cMRF have clear effects on vergence movements (Chaturvedi and Van Gisbergen 1999, 2000; Luque et al. 2006; Suzuki et al. 2004; Waitzman et al. 2007). Consistent with these findings are the recent reports that cMRF neurons dynamically encode the movement of an individual eye (Waitzman et al. 2007) and SC neuronal activity is altered when saccades are accompanied by vergence (Walton and Mays 2003). Because the modulation of primate SC neurons was observed to be more robust for purely conjugate than disconjugate saccades, it has been suggested that the SC is not tuned in three dimensions (Walton and Mays 2003). However, given that *1*) the SC has strong anatomical connections to saccadic neurons in the PPRF and cMRF (Moschovakis et al. 1988) and *2*) neurons in both of these regions have been found to dynamically encode the movement of an individual eye (present study, Waitzman et al. 2007) it is suggested that neurons in the SC should be reexamined for evidence of an individual eye command.

Another possible source of vergence inputs to SBNs is the fastigial nucleus of the cerebellum. This nucleus projects directly to the SBN region (Noda et al. 1990) and contains neurons with saccade-related activity (Fuchs et al. 1993). Although it is not known whether these neurons encode vergence modulations during disconjugate saccades, neurons in the adjacent interposed nucleus can carry vergence and disparity information (Zhang and Gamlin 1998). Finally, it is also possible that brain stem vergence-velocity or near-response neurons could project to the SBN region. However, there is currently no evidence available to support this projection (Gamlin 1999). Future studies of vergence–saccade interactions in other brain areas are required for further testing of this framework.

ACKNOWLEDGMENTS

We thank D. M. Waitzman, S. Sadeghi, and J. Brooks for critically reading the manuscript and B. G. Lippert, J. Knowles, and W. Kucharski for excellent technical assistance.

GRANTS

This study was supported by the Canadian Institutes of Health Research, the Natural Science and Engineering Research Council of Canada, and the Fonds de la Recherche en Santé du Québec.

REFERENCES

Busettini C, Mays LE. Pontine omnipause activity during conjugate and disconjugate eye movements in macaques. *J Neurophysiol* 90: 3838–3853, 2003.

Busettini C, Mays LE. Saccade–vergence interactions in macaques. I. Test of the omnipause Multiply Model. *J Neurophysiol* 94: 2295–2311, 2005a.

Busettini C, Mays LE. Saccade–vergence interactions in macaques. II. Vergence enhancement as the product of a local feedback vergence motor error and a weighted saccadic burst. *J Neurophysiol* 94: 2312–2330, 2005b.

Carpenter J, Bithell J. Bootstrap confidence intervals: when, which, what? A practical guide for medical statisticians. *Stat Med* 19: 1141–1164, 2000.

Chaturvedi V, Van Gisbergen J. Perturbation of combined saccade–vergence movements by microstimulation in monkey superior colliculus. *J Neurophysiol* 81: 2279–2296, 1999.

Chaturvedi V, Van Gisbergen J. Stimulation in the rostral pole of monkey superior colliculus: effects on vergence eye movements. *Exp Brain Res* 132: 72–78, 2000.

Collewijn H, Erkelens CJ, Steinman RM. Voluntary binocular gaze-shifts in the plane of regard: dynamics of version and vergence. *Vision Res* 35: 3335–3358, 1995.

Collewijn H, Erkelens CJ, Steinman RM. Trajectories of the human binocular fixation point during conjugate and non-conjugate gaze-shifts. *Vision Res* 37: 1049–1069, 1997.

Cova A, Galiana H. Providing distinct vergence and version dynamics in a bilateral oculomotor network. *Vision Res* 35: 3359–3371, 1995.

Cova A, Galiana H. A bilateral model integrating vergence and the vestibulo-ocular reflex. *Exp Brain Res* 107: 435–452, 1996.

Crawford JR, Howell DC, Garthwaite PH. Payne and Jones revisited: estimating the abnormality of test score differences using a modified paired samples t test. *J Clin Exp Neuropsychol* 20: 898–905, 1998.

Cullen K, Guitton D. Analysis of primate IBN spike trains using system identification techniques. II. relationship to gaze, eye, and head movement dynamics during head-free gaze shifts. *J Neurophysiol* 78: 3283–3306, 1997b.

Cullen K, Guitton D, Rey C, Jiang W. Gaze-related activity of putative inhibitory burst neurons in the head-free cat. *J Neurophysiol* 70: 2678–2683, 1993b.

Cullen K, McCrea R. Firing behavior of brain stem neurons during voluntary cancellation of the horizontal vestibuloocular reflex. I. Secondary vestibular neurons. *J Neurophysiol* 70: 828–843, 1993.

Cullen KE, Chen-Huang C, McCrea RA. Firing behavior of brain stem neurons during voluntary cancellation of the horizontal vestibuloocular reflex. II. Eye movement related neurons. *J Neurophysiol* 70: 844–856, 1993.

Cullen KE, Guitton D. Inhibitory burst neuron activity encodes gaze, not eye, metrics and dynamics during passive head on body rotation. Evidence that vestibular signals supplement visual information in the control of gaze shifts. *Ann NY Acad Sci* 781: 601–606, 1996.

Cullen KE, Guitton D. Analysis of primate IBN spike trains using system identification techniques. I. Relationship to eye movement dynamics during head-fixed saccades. *J Neurophysiol* 78: 3259–3282, 1997.

Cullen KE, Rey CG, Guitton D, Galiana HL. The use of system identification techniques in the analysis of oculomotor burst neuron spike train dynamics. *J Comput Neurosci* 3: 347–368, 1996.

Eckmiller R, Blair S, Westheimer G. Fine structure of saccade bursts in macaque pontine neurons. *Brain Res* 181: 460–464, 1980.

Eckmiller R, Mackeben M. Pre-motor single unit activity in the monkey brain stem correlated with eye velocity during pursuit. *Brain Res* 184: 210–214, 1980.

Enright J. Changes in vergence mediated by saccades. *J Physiol* 350: 9–31, 1984.

Enright JT. The remarkable saccades of asymmetrical vergence. *Vision Res* 32: 2261–2276, 1992.

Erkelens CJ, Van der Steen J, Steinman RM, Collewijn H. Ocular vergence under natural conditions. I. Continuous changes of target distance along the median plane. *Proc R Soc Lond B Biol Sci* 236: 417–440, 1989.

Ferraina S, Paré M, Wurtz R. Disparity sensitivity of frontal eye field neurons. *J Neurophysiol* 83: 625–629, 2000.

Fuchs AF, Robinson DA. A method for measuring horizontal and vertical eye movements in the monkey. *J Physiol* 191: 609–631, 1966.

Fuchs AF, Robinson DA, Straube A. Role of the caudal fastigial nucleus in saccade generation. I. Neuronal discharge pattern. *J Neurophysiol* 70: 1723–1740, 1993.

Gamlin PD. Subcortical neural circuits for ocular accommodation and vergence in primates. *Ophthalmic Physiol Opt* 19: 81–89, 1999.

Gamlin PD, Gnadt JW, Mays LE. Abducens internuclear neurons carry an inappropriate signal for ocular convergence. *J Neurophysiol* 62: 70–81, 1989.

Gamlin PD, Yoon K. An area for vergence eye movement in primate frontal cortex. *Nature* 407: 1003–1007, 2000.

Gnadt JW, Beyer J. Eye movements in depth: what does the monkey's parietal cortex tell the superior colliculus? *Neuroreport* 9: 233–238, 1998.

Gnadt JW, Gamlin PD, Mays LE, Zhang Y. Vergence-related cells near the abducens nuclei. *Soc Neurosci Abstr* 14: 612, 1988.

Hayes AV, Richmond BJ, Optican LM. A UNIX-based multiple process system for real-time data acquisition and control. In: *Proceedings of the Western Electronic Show and Conference (Wescon/82), Anaheim, California, Sept. 15, 1982*. El Segundo, CA: Electronic Conventions, 1982, p. 2/1-1–2/1-10.

Hazel T, Sklavos S, Dean P. Estimation of premotor synaptic drives to simulated abducens motoneurons for control of eye position. *Exp Brain Res* 146: 184–196, 2002.

Hepp K, Henn V. Spatio-temporal recoding of rapid eye movement signals in the monkey paramedian pontine reticular formation (PPRF). *Exp Brain Res* 52: 105–120, 1983.

Highstein SM, Baker R. Excitatory termination of abducens internuclear neurons on medial rectus motoneurons: relationship to syndrome of internuclear ophthalmoplegia. *J Neurophysiol* 41: 1647–1661, 1978.

Judge SJ, Richmond BJ, Chu FC. Implantation of magnetic search coils for measurement of eye position: an improved method. *Vision Res* 20: 535–538, 1980.

Kaneko CR, Evinger C, Fuchs AF. Role of cat pontine burst neurons in generation of saccadic eye movements. *J Neurophysiol* 46: 387–408, 1981.

Keller EL. Participation of medial pontine reticular formation in eye movement generation in monkey. *J Neurophysiol* 37: 316–332, 1974.

Kenyon R, Ciuffreda K, Stark L. Unequal saccades during vergence. *Am J Optom Physiol Opt* 57: 586–594, 1980.

King WM, Zhou W. New ideas about binocular coordination of eye movements: is there a chameleon in the primate family tree? *Anat Rec* 261: 153–161, 2000.

King WM, Zhou W. Neural basis of disjunctive eye movements. *Ann NY Acad Sci* 956: 273–283, 2002.

Kumar AN, Han Y, Dell'Osso LF, Durand DM, Leigh RJ. Directional asymmetry during combined saccade–vergence movements. *J Neurophysiol* 93: 2797–2808, 2005.

Kumar AN, Han YH, Kirsch RF, Dell'Osso LF, King WM, Leigh RJ. Tests of models for saccade–vergence interaction using novel stimulus conditions. *Biol Cybern* 95: 143–157, 2006.

Langer TP, Kaneko CR, Scudder CA, Fuchs AF. Afferents to the abducens nucleus in the monkey and cat. *J Comp Neurol* 245: 379–400, 1986.

Leigh RJ, Zee DS. *The Neurology of Eye Movements*. New York: Oxford Univ. Press, 1999, p. 286–320.

Luque MA, Perez-Perez MP, Herrero L, Waitzman DM, Torres B. Eye movements evoked by electrical microstimulation of the mesencephalic reticular formation in goldfish. *Neuroscience* 137: 1051–1073, 2006.

Luschei E, Fuchs AF. Activity of brain stem neurons during eye movements of alert monkeys. *J Neurophysiol* 35: 445–461, 1972.

Maxwell JS, King WM. Dynamics and efficacy of saccade-facilitated vergence eye movements in monkeys. *J Neurophysiol* 68: 1248–1260, 1992.

Mays LE, Gamlin PD. Neuronal circuitry controlling the near response. *Curr Opin Neurobiol* 5: 763–768, 1995.

Mays LE, Porter JD. Neural control of vergence eye movements: activity of abducens and oculomotor neurons. *J Neurophysiol* 52: 743–761, 1984.

Mays LE, Porter JD, Gamlin PD, Tello CA. Neural control of vergence eye movements: neurons encoding vergence velocity. *J Neurophysiol* 56: 1007–1021, 1986.

McConville KM, Tomlinson D, King WM, Paige GD, Na E-Q. Eye position signals in the vestibular nuclei: consequences for models of integrator function. *J Vestib Res* 4: 391–400, 1994.

McFarland J, Fuchs A. Discharge patterns in nucleus prepositus hypoglossi and adjacent medial vestibular nucleus during horizontal eye movement in behaving macaques. *J Neurophysiol* 68: 319–332, 1992.

Moschovakis AK, Karabelas AB, Highstein SM. Structure–function relationships in the primate superior colliculus. II. Morphological identity of presaccadic neurons. *J Neurophysiol* 60: 263–302, 1988.

Noda H, Sugita S, Ikeda Y. Afferent and efferent connections of the oculomotor region of the fastigial nucleus in the macaque monkey. *J Comp Neurol* 302: 330–348, 1990.

Ono H, Nakamizo S, Steinbach MJ. Nonadditivity of vergence and saccadic eye movement. *Vision Res* 18: 735–739, 1978.

Oohira A. Vergence eye movements facilitated by saccades. *Jpn J Ophthalmol* 37: 400–413, 1993.

Press LJ. Effect of VDUs on the eyes. *Optom Vis Sci* 74: 130–131, 1997.

Ramat S, Somers JT, Das VE, Leigh RJ. Conjugate ocular oscillations during shifts of the direction and depth of visual fixation. *Invest Ophthalmol Vis Sci* 40: 1681–1686, 1999.

Robinson DA. Models of the saccadic eye movement control system. *Kybernetik* 14: 71–83, 1973.

Roy JE, Cullen KE. Vestibuloocular reflex signal modulation during voluntary and passive head movements. *J Neurophysiol* 87: 2337–2357, 2002.

Roy JE, Cullen KE. Brain stem pursuit pathways: dissociating visual, vestibular, and proprioceptive inputs during combined eye-head gaze tracking. *J Neurophysiol* 90: 271–290, 2003.

Schiller PH, Stryker M. Single-unit recording and stimulation in superior colliculus of the alert rhesus monkey. *J Neurophysiol* 35: 915–924, 1972.

Scudder CA. A new local feedback model of the saccadic burst generator. *J Neurophysiol* 59: 1455–1475, 1988.

Scudder CA, Fuchs AF. Physiological and behavioral identification of vestibular nucleus neurons mediating the horizontal vestibuloocular reflex in trained rhesus monkeys. *J Neurophysiol* 68: 244–264, 1992.

Scudder CA, Fuchs AF, Langer TP. Characteristics and functional identification of saccadic inhibitory burst neurons in the alert monkey. *J Neurophysiol* 59: 1430–1454, 1988.

Scudder CA, Kaneko CRS, Fuchs AF. The brainstem burst generator for saccadic eye movements: a modern synthesis. *Exp Brain Res* 142: 439–462, 2002.

Sokal RR, Rohlf FJ. *Biometry: The Principles and Practice of Statistics in Biological Research*. New York: Freeman, 1995, p. xix.

Strassman A, Highstein SM, McCrea RA. Anatomy and physiology of saccadic burst neurons in the alert squirrel monkey. I. Excitatory burst neurons. *J Comp Neurol* 249: 337–357, 1986a.

Strassman A, Highstein SM, McCrea RA. Anatomy and physiology of saccadic burst neurons in the alert squirrel monkey. II. Inhibitory burst neurons. *J Comp Neurol* 249: 358–380, 1986b.

Suzuki S, Suzuki Y, Ohtsuka K. Convergence eye movements evoked by microstimulation of the rostral superior colliculus in the cat. *Neurosci Res* 49: 39–45, 2004.

Sylvestre PA, Choi JT, Cullen KE. Discharge dynamics of oculomotor neural integrator neurons during conjugate and disjunctive saccades and fixation. *J Neurophysiol* 90: 739–754, 2003.

Sylvestre PA, Cullen KE. Quantitative analysis of abducens neuron discharge dynamics during saccadic and slow eye movements. *J Neurophysiol* 82: 2612–2632, 1999.

Sylvestre PA, Cullen KE. Dynamics of abducens nucleus neuron discharges during disjunctive saccades. *J Neurophysiol* 88: 3452–3468, 2002.

Sylvestre PA, Galiana HL, Cullen KE. Conjugate and vergence oscillations during saccades and gaze shifts: implications for integrated control of binocular movement. *J Neurophysiol* 87: 257–272, 2002.

Van Gisbergen JA, Robinson DA, Gielen S. A quantitative analysis of generation of saccadic eye movements by burst neurons. *J Neurophysiol* 45: 417–442, 1981.

Van Opstal A, Van Gisbergen J, Eggermont J. Reconstruction of neural control signals for saccades based on an inverse method. *Vision Res* 25: 789–801, 1985.

Wackerly DD, Mendenhall W, Scheaffer RL. *Mathematical Statistics with Applications.* Belmont, CA: Duxbury Press, 1996, p. xvi.

Waitzman DM, Van Horn M, Cullen KE. Evidence for independent control of saccadic eye movement in the primate central mesencephalic reticular formation (cMRF). *Soc Neurosci Abstr* 33: 718, 2007.

Walton MM, Mays LE. Discharge of saccade-related superior colliculus neurons during saccades accompanied by vergence. *J Neurophysiol* 90: 1124–1139, 2003.

Yoshida K, McCrea R, Berthoz A, Vidal PP. Morphological and physiological characteristics of inhibitory burst neurons controlling horizontal rapid eye movements in the alert cat. *J Neurophysiol* 48: 761–784, 1982.

Zee DS, Fitzgibbon EJ, Optican LM. Saccade–vergence interactions in humans. *J Neurophysiol* 68: 1624–1641, 1992.

Zhang H, Gamlin PD. Neurons in the posterior interposed nucleus of the cerebellum related to vergence and accommodation. I. Steady-state characteristics. *J Neurophysiol* 79: 1255–1269, 1998.

Zhang Y, Mays LE, Gamlin PD. Characteristics of near response cells projecting to the oculomotor nucleus. *J Neurophysiol* 67: 944–960, 1992.

Zhou W, King WM. Premotor commands encode monocular eye movements. *Nature* 393: 692–695, 1998.

Zuber B, Semmlow J, Stark L. Frequency characteristics of the saccadic eye movement. *Biophys J* 8: 1288–1298, 1968.